Advanced Physical Research
Vol.8, No.1, 2026, pp.130-139
https://doi.org/10.62476/apr.81130

MODELING THE FRESNEL ZONE OF A CIRCULAR TRANSDUCER

Islam J. Islamov[1*], **Kalin S. Kalinov**[2], **Iliyan Y. Iliev**[2],
Ramil G. Akhundov[3], **Vagif A. Gasimov**[1], **Boyan K. Mednikarov**[2],
Miroslav Y. Tsvetkov[2], **M.A. Abdullayev**[4]

[1]Baku Engineering University, Baku, Azerbaijan
[2]Nikola Vaptsarov Naval Academy, Varna, Bulgaria
[3]National Defense University, Baku, Azerbaijan
[4]Azerbaijan Technological University, Ganja, Azerbaijan

Abstract. In classic acoustics one differs two areas around the acoustic source – near field and far field. There is a third area, called very near field, but it is mostly the subject of researches in the field of vibration mechanics. The near and the far field are often called Fresnel zones and Fraunhofer zone. In this work a criterion for determining the borders of Fresnel zones is proposed. The criterion is based on multiple examinations, researches and measurements of the spatial parameters and characteristics and some of the electrical parameters and characteristics of circular transducers (loudspeakers). From the presented theoretical and experimental review of the Fresnel zones one can conclude: the bigger the transducer radius, the longer the Fresnel zones; the higher the frequency, the longer the Fresnel zones; the higher the wavelength, the shorter the Fresnel zones; the higher the sound speed, the shorter the Fresnel zones.

Keywords: Circular transducer, near field, far field, Fresnel zones, Rayleigh integral.
Corresponding author: I.J. Islamov, Baku Engineering University, Hasan Aliyev str., 120, AZ 0101, Baku, Azerbaijan, Tel.: +994 50 626 76 99, e-mail: *isislamov@beu.edu.az*
Received: 8 October 2025; Revised: 7 November 2025; Accepted: 12 December 2025;
Published: 18 February 2026.

1 Introduction

In order to gain deeper understanding of the nature of the sound field created by a transducer it is necessary to examine its spatial characteristics. Sound pressure p_a is the physical quantity (parameter) that gives detailed information about the sound field. Hence, in order to understand the physics of the sound field it is necessary to calculate the sound pressure level (SPL), created by transducers with different geometry (rectangular, circular, elliptical etc.), for each point of space.

In classic acoustics one differs two areas around the acoustic source – near field and far field. There is a third area, called very near field, but it is mostly the subject of researches in the field of vibration mechanics. In many references near field is called Fresnel zones and far field is called Fraunhofer zone. For each zone there are different theoretical formulas for determining the sound pressure p_a.

In this work a criterion for determining the borders of Fresnel zones is proposed. The criterion is based on a multitude of examinations, researches and measurements of the spatial parameters and characteristics (Iliev et al., 2014; Iliev, 2013; Sirakov & Iliev, 2013) and some of the electrical parameters and characteristics (Zhivomirov & Iliev , 2015) of circular transducers (loudspeakers).

The criterion uses a normalized difference between two formulas – one for calculating the on-axis total acoustic sound pressure p_{aTotal} and the other for calculating the on-axis sound pressure in the far field p_{aFar}.

2 Theoretical background

One can calculate the acoustic pressure p_a created by the circular transducer by Huyghens-Fresnel dependence, known in acoustics as Rayleigh integral (Lependin, 1978; Rschevkin, 1960; Kleiner, 2013):

$$p_a(\theta, f, r, t) = j\rho_s f v_m \int_Q^{\infty} \frac{1}{y} e^{j(\omega t - ky)} dQ, \tag{1}$$

where θ is directivity angle (elevation); $f-$ transducer frequency; $r-$ distance between the transducer and the observation point (where the sound pressure is measured); ρ_s- density of the environment; v_m-piston amplitude; $Q-$surface of the transducer; $y-$ distance between elementary section (point source) and observation point; ω – angular frequency; $k = \frac{2\pi}{\lambda}-$ wave number; $\lambda-$ wavelength.

In Iliev (2014) a modified expression for calculating the total acoustic pressure p_{aTotal} is proposed:

$$p_{aTotal}(\theta, f, r) = \rho_s f v_m e^{j\omega t} \int_0^a x dx \int_0^{2\pi} \frac{e^{-j\frac{2\pi f}{c}\left(\sqrt{r^2+x^2+2rxsin\theta cos\alpha}\right)}}{\sqrt{r^2+x^2+2rxsin\theta cos\alpha}} d\alpha, \tag{2}$$

where a is a circular transducer radius; x – the radial distance between the elementary section (point source) and center of the circular transducer; c – speed of sound; α - directivity angle (azimuth).

For the far field, when the distance r is significantly larger than the diameter of the transducer d ($r \gg d$) the acoustic pressure p_{aFar} is (Rschevkin, 1960):

$$p_{aFar}(\theta, f, r) = \frac{\rho_s f v_m}{r} e^{j\omega t} \int_0^{\alpha} x dx \int_0^{2\pi} e^{-j\frac{2\pi f}{c}(r + xsin\theta cos\alpha)} d\alpha. \tag{3}$$

Eq. (3) is also known as Fraunhofer solution of the Rayleigh integral. For the near field the acoustic pressure amplitude p_a on the axis of the transducer (Eqs. (1) and (2)) can be simplified (Lependin, 1978; Rschevkin, 1960):

$$p_a(0, f, r) = 2\rho_s \left| sin\left\{\frac{\pi f}{c}\left[\sqrt{r^2+a^2} - r\right]\right\}\right|. \tag{4}$$

Eq. (4) is a kind of on-axis Fresnel solution of the Rayleigh integral. Study of Eq. (4) reveals that the axial acoustic pressure extremes occur (because of the sine function) at (Iliev, 2013; Lependin, 1978; Rschevkin, 1960):

$$\frac{\pi f}{c}\left[\sqrt{r^2+a^2} - r\right] = m\pi, \ m = 0, 1, 2 \ldots \tag{5}$$

Furthermore, the solution of the above expression gives the values of r at the SPL extremes (Lependin, 1978):

$$r_m = \frac{a^2}{m\lambda} - \frac{m\lambda}{4}. \tag{6}$$

Subsequently, if one moves toward the sound source from a given distance r, the first SPL maximum will be encountered at:

$$r_1 = \frac{a^2}{\lambda} - \frac{\lambda}{4}. \tag{7}$$

The first minimum in the SPL will appear at:

$$r_2 = \frac{a^2}{2\lambda} - \frac{\lambda}{2}. \quad (8)$$

For distances $r< r_1$ the acoustic field in the immediate proximity of the transducer is complicated (because of the SPL minimums and maximums). These extremes are typical for the Fresnel zones because the axial sound pressure p_a displays strong interference effects.

For distances $r> r_1$ the character of the axial sound pressure p_a decreases monotonically, approaching an asymptotic dependence $1/r$ (Kleiner, 2013; Gelfand, 2005) (Fraunhofer zone). The distance r_1 could be accepted as a reasonable upper border of Fresnel zones or as a border between Fresnel zones and Fraunhofer zone. This distance manipulation of Eq. (7)):

$$f_{min} > \frac{c}{2a}. \quad (9)$$

From Eq. (9) it is obvious that at frequencies lower that f_{min} the radiation of the transducer will be similar to the radiation of a simple source (there will be no Fresnel zones) (Yuning, 2025; Ganti et al., 2023; Zhong et al., 2024; Yu et al., 2024; Cao et al., 2025; Xiong et al., 2025).

It should be noted that different authors (Smith, 1997; Urban et al., 2003) have proposed various expressions (similar to Eq. (7) which gives the last maximum, perceived by some as the upper border distance of the near field). In Kozien (2012) the hybrid intensity method is used for determining the border between near and far field (Fresnel zones and Fraunhofer zones).

Those methods have some disadvantages. The first, used in Smith (1997), Urban et al. (2003), Islamov & Aslanzadeh (2023), Islamov et al. (2025) are too rough and not so accurate. The method used in Kozien (2012) is too complicated and much less practical.

3 Solution of the problem

The boundary between the Fresnel and Fraunhofer zones can be determined by the condition that Fresnel diffraction is observed at a finite distance from the obstacle (in the near zone), and Fraunhofer diffraction is observed at an infinite distance from the obstacle (in the far zone).

Modeling a loudspeaker's Fresnel zone is based on the Huygens-Fresnel principle, which states that each point on the loudspeaker's surface (the wave source) is the center of secondary spherical waves. The modeling involves dividing the wavefront into annular zones, since vibrations from adjacent zones, spaced a half-wave apart, cancel each other out through interference.

In this paper the author proposes a method for determining the border between the Fresnel zones and the Fraunhofer zone similar to those used for determining the spectral density of a rectangular pulse train or RC-circuit time constant. Based on the normalized difference between Eq. (2) and Eq. (3):

$$\Delta p_a\left(\theta, f, r\right) = \frac{p_{aTotal-}p_{aFar}}{p_{aFar}} \cdot 100, \quad (10)$$

This one can define the upper frequency $f_{maxFrensel}$ limit of the Fresnel zones (the moment when both of the expressions become similar) for a given loudspeaker (with a given radius a). The frequency range of the loudspeaker must be also taken into account.

For instance, the axial sound pressure in the far field p_{aFar} created by the loudspeaker with radius $arm = 0.08\ m$ is shown in Fig. 1.

The total axial sound pressure p_{aTotal} created by the same loudspeaker is shown in Fig. 2.

The normalized difference between the calculated SPL by Eq. (2) and the SPL calculated by Eq. (3) is shown in Fig. 3. The same correlation in percentage is presented in Fig. 4.

The normalized difference between the total sound pressure level and the far-field sound pressure level of a circular transducer is the relative difference between the integrated (total) sound energy level emitted by the transducer and the sound pressure level measured at a certain

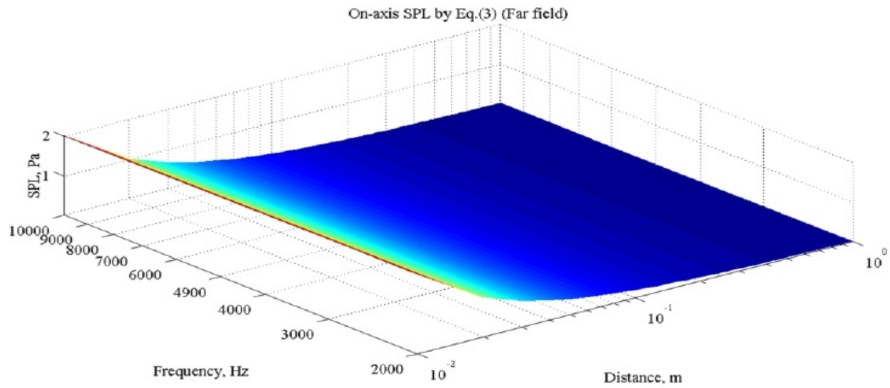

Figure 1: Axial far-field sound pressure level of a circular transducer according to Eq. (3)

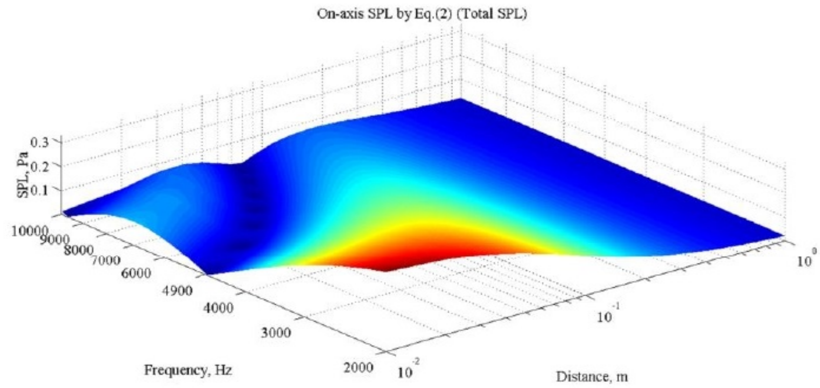

Figure 2: Total far-field sound pressure level of a circular transducer according to Eq. (2)

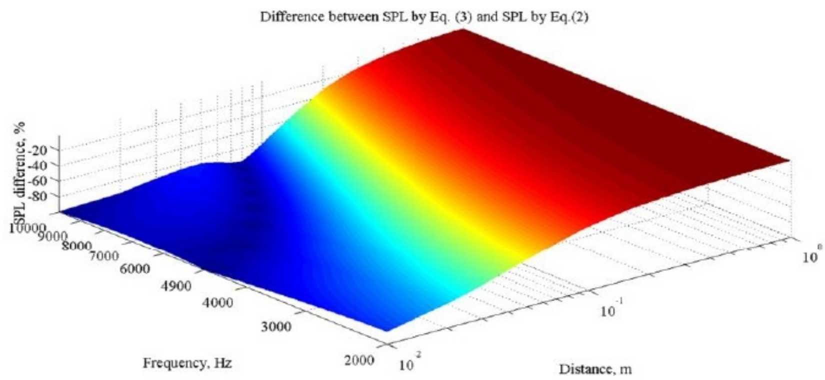

Figure 3: The normalized difference between the total sound pressure and the far-field sound pressure of a circular transducer according to Eq. (10)

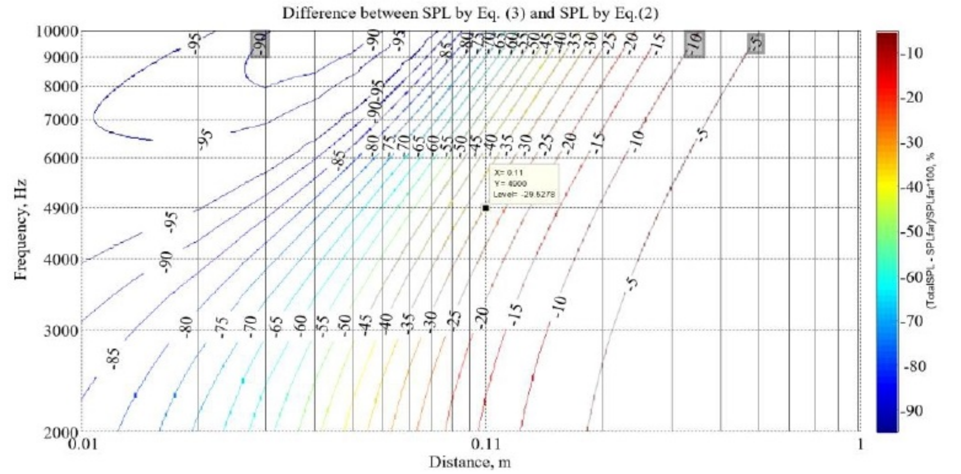

Figure 4: The normalized difference between the overall sound pressure level and the far-field sound pressure level of the circular transducer according to Eq. (10) – in percent

distance in the far-field, which is typically an important parameter in the design and analysis of acoustic systems. This difference is defined as the ratio of the total sound pressure level to the far-field sound pressure level. The lines in Fig. 4 are not isolines, as these lines do not connect points with the same values of any quantity.

Fig. 4. reveals that the Fresnel zones will exists only for some frequencies f and some distances r. The author proposes the moment when $\Delta p_a < 30\%$ to be considered an upper limit border of the Fresnel zones (similar to half power point – 0.707).

4 Experimental results

The practical measurements were carried out with a DAQ system, a laptop, a sound-level meter, loudspeaker (radius $a = 0.08\ m$) and software product for SPL measuring (Iliev et al., 2014). During the experiments the temperature and the intrinsic noise level in the anechoic chamber were measured with professional environment meter as follows: $t = 19.7°C$, intrinsic noise level – 26.8 dB.

The goal of the presented measurements is to show pattern and to gives a semiquantitative, intuitive understanding of the proposed criterion, not to claim for accuracy. More precise results must be obtained using numerical analysis techniques or finite element analysis.

For the loudspeaker at hand, one observes the Fresnel zones between frequencies $f_{min} > 2147\ Hz$ (by Eq. (9)) and its upper frequency range (in this case approximately $f_{max} = f_{maxFrensel} = 10000 Hz$ Iliev et al. (2013)). Furthermore, for distances larger than $r > 0.065\ m$ for $f = 2200\ Hz$ and $r > 0.21\ m$ for $f = 10000 Hz$ (Fig. 4) the sound pressure p_a drops monotonically, therefore there is a Fraunhofer zone.

Theoretical frequency response at distance $r = 0.012\ m$ is shown in Fig. 5. The plot is a slide of a 3D plot in Fig. 2. A minimum at frequency f= 4900 Hz for that distance $r = 0.012\ m$ is clearly noticeable.

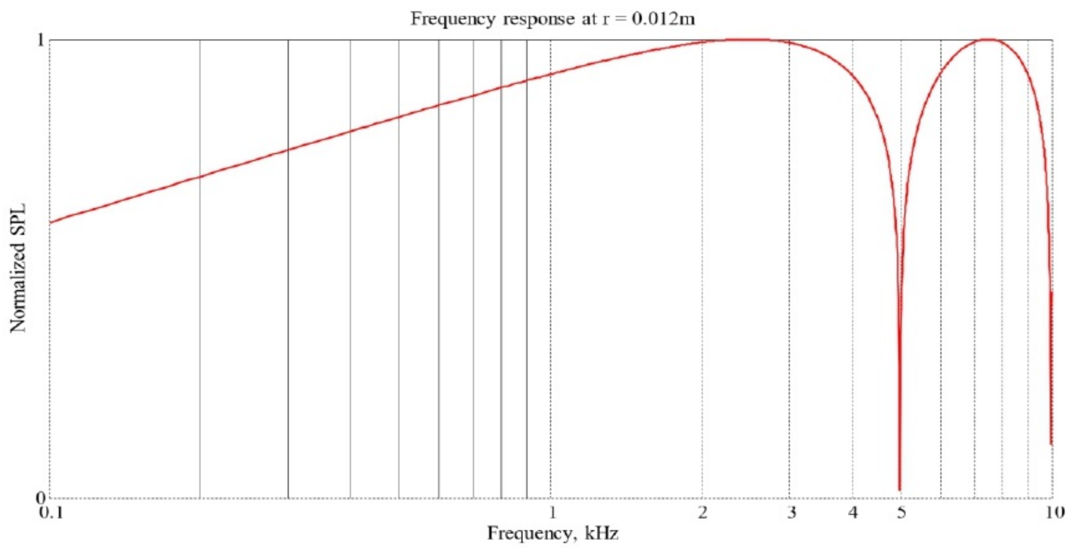

Figure 5: Theoretical frequency response at distance $r = 0.012\ m$

In Fig. 6 the measured loudspeaker's frequency response at distance $r = 0.012\ m$ is presented.

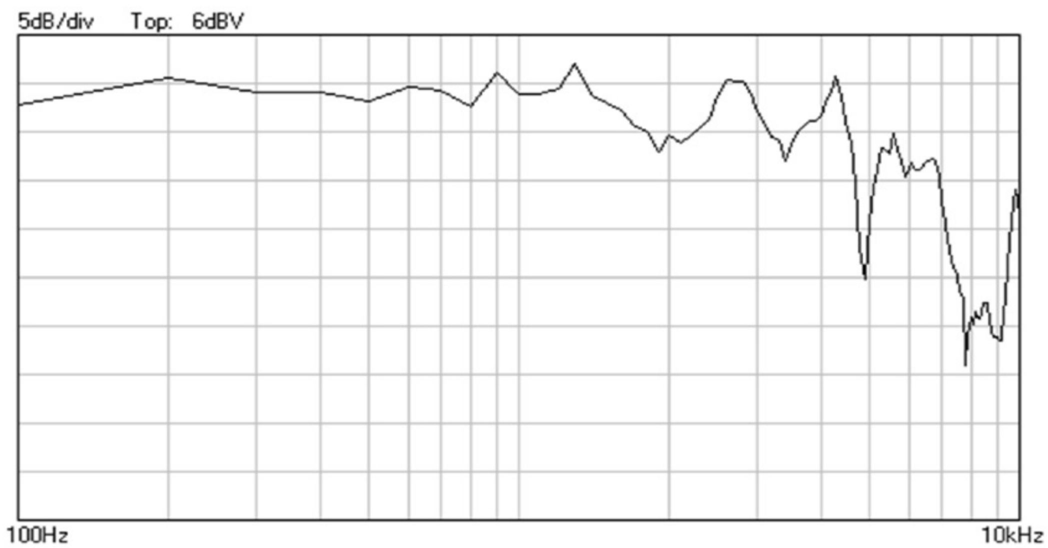

Figure 6: Measured frequency response at $r = 0.012m$

In Fig. 6 one can notice the sharp minimums and maximums in the frequency response for frequencies $f > 2147\ Hz$. Some of those extremes are caused by the interferences in the Fresnel zones (i.e. the sharp minimum at frequency $f = 4900\ Hz$ marked with red circle).

To express the asymptotic form of the SPL in the far field (in the Fraunhofer zone) the frequency response of a loudspeaker (radius $a = 0.08\ m$) at six different distances is measured (Fig. 7). The SPL for frequency $f = 4900\ Hz$ from all of the six measurements are visualized in Fig. 8.

Loudspeaker type: BS-634T. Loudspeaker calibration is the process of determining and aligning its actual metrological parameters (such as sound pressure, frequency response, etc.) with established standards using reference equipment. Specialized, certified laboratories and comparators are used for precise calibration.

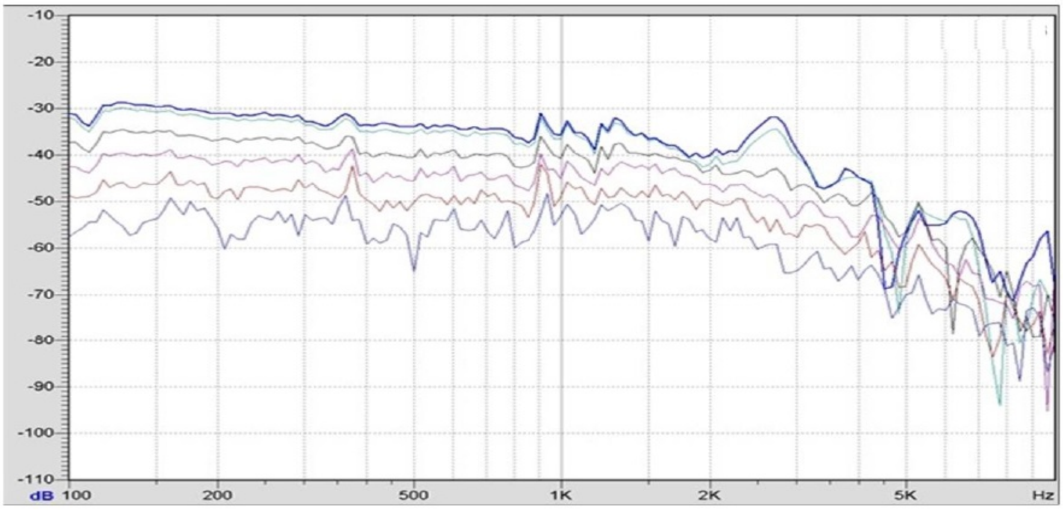

Figure 7: Measured frequency response at distances: $r = (0.002\ m, 0.012\ m, 0.06\ m, 0.12\ m, 0.24\ m, 0.48\ m)$

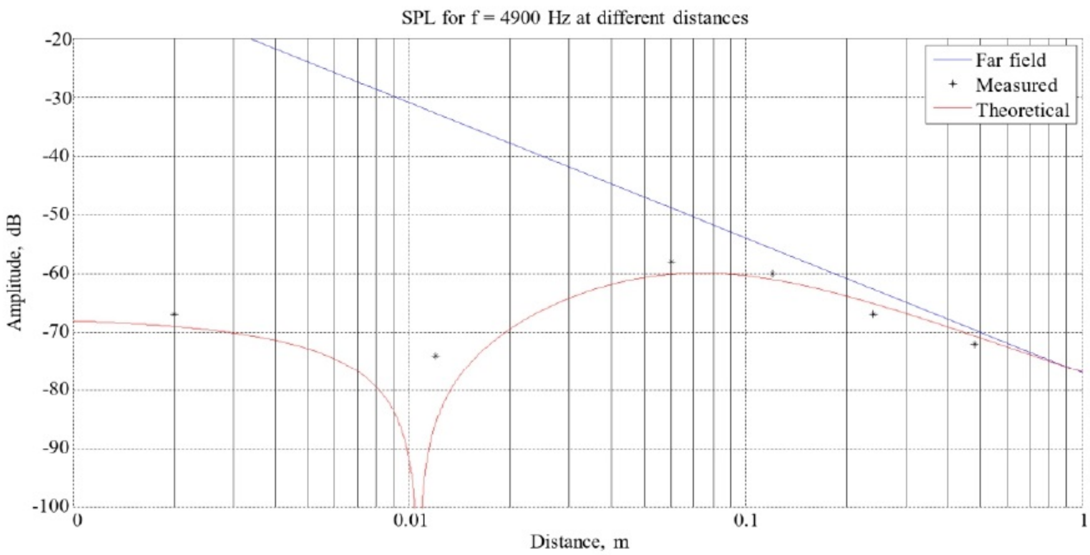

Figure 8: SPL for frequency $f = 4900\ Hz$, at distances: $r = (0.002\ m, 0.012\ m, 0.06\ m, 0.12\ m, 0.24\ m, 0.48\ m)$

The actual calibration process follows a pre-determined plan. The measuring device being calibrated is compared to a reference standard. Measurements are taken at various points across the device's entire measurement range. The number of measurement points depends on the device type and calibration requirements. Each measurement point is measured multiple times to capture any random variations. During the calibration process, all relevant data is carefully recorded. This includes the measured values themselves, as well as environmental conditions and any deviations from the norm. Calibration is performed under strictly controlled conditions to minimize interference. Particular attention is paid to maintaining the prescribed waiting intervals between measurements to account for thermal effects.

The following conditions are accepted when determining the measurement error: 1. The error of the measurement method shall be no more than $\pm 2\ dB$. 2. The total error of the measuring instruments shall be no more than: ± 2 dB - at frequencies up to 100 Hz; ± 1.5 dB - in the frequency range above 100 to 315 Hz; ± 1 dB - at frequencies above 315 Hz. 3. The total error of measuring the sound pressure of the loudspeaker shall be no more than: ± 3.0 dB - at frequencies up to 100 Hz; ± 2.5 dB - in the frequency range above 100 to 315 Hz; ± 2.0 dB - at frequencies above 315 Hz. 4. The total error of measurements when determining electrical characteristics shall be no more than ± 0.5 dB.

5 Conclusion

The experimentally obtained minimum in the SPL for frequency f=4900 Hz (Fig. 6) is theoretically predicted by Fresnel solution (Fig. 5). For a given circular acoustic transducer the Fresnel zones appear for some frequencies f at some distances r.

In Fig. 8 one can notice the overlaps between the measured SPL and the theoretical SPL for frequency f=4900 Hz. For relatively large distances r the theoretical SPL and the experimental SPL decrease monotonically, approaching an asymptotic dependence $1/r$ (typical for Fraunhofer zone).

If one applies the proposed criterion for a loudspeaker with radius $a = 0.08$ m, one will observe the Fresnel zones between frequencies $f_{minFrensel}$> 2147 Hz and the upper frequency range of the loudspeaker. After applying 30% difference between the SPL calculated by Eq. (2) and the SPL calculated by Eq. (3) one can acquire the distance r of the Fresnel zones (frequency dependent). Thus, for frequency f=4900 Hz by means of the isobars from Fig. 4 the Fresnel zones exists only for distances $r < 0.11$ m, for frequency f=2200 Hz the Fresnel zones exists for distances $r < 0.065$ m, etc.

The proposed criterion for determining the border between the Fresnel zones and Fraunhofer zone is simple, easy to use and gives relatively accurate results. If one knows the radius a and the frequency f of the transducer (loudspeaker) one can implement Eq. (10) and acquire graph similar to those in Fig. 4. By means of isobars one can choose specific conditions for stating the border between the Fresnel zones and the Fraunhofer zone (different from $\Delta p_a < 30\%$).

From the presented theoretical and experimental review of the Fresnel zones one can conclude:

- the bigger the transducer radius a , the longer the Fresnel zones;
- the higher the frequency f, the longer the Fresnel zones;
- the higher the wavelength λ, the shorter the Fresnel zones;
- the higher the sound speed c, the shorter the Fresnel zones.

6 Acknowledgement

The authors express their deep gratitude to the entire editorial board of the journal for their professionalism and excellent work. I especially want to note the very careful and attentive attitude of the reviewers, and their detailed study of the manuscript of the article. Their comments and recommendations are constructive, which allows for improving the quality of the presented research and structuring of the article as much as possible according to the requirements of the journal. The friendly and prompt nature of communication with the editorial board contributes to the rapid resolution of all emerging issues and compliance with the stated deadlines for reviewing and publishing the article.

This research paper has received funding from Ministry of Education and Science of the Republic of Bulgaria under the National Science Program “SECURITY AND DEFENSE”, in implementation of the Decision of the Council of Ministers of the Republic of Bulgaria No: 731/21.10.2021 and according to Agreement No: D01-74/19.05.2022.

References

Cao, Y., Quan, J., Sun, B., Fang, X., Hang, Z., Gao, L., ... & Xu, Y. (2024). Arbitrary multi-directional acoustic beam emission from a cylindrical metasurface with grafted topological charge. *Applied Physics Letters, 124*(13).

Ganti A., Martinez M., Hickman G., & Krolik J. (2023). A wavefront adaptive sensing beamformer for ocean acoustic waveguides. *J. Acoustical Soc. Am.*, 154, 2398-2409.

Gelfand S. (2005). *Hearing,* Taylor & Francis, 11-12.

Iliev I. (2014). *Polar Response of a Circular Piston.* TEM Journal, *3*(3), 230-234.

Iliev I., Sirakov E., & Zhivomirov H. (2013). Sound Near Field Examination of a Circular Piston. *UNITECH'2013, Gabrovo, Bulgaria. Conference Proceedings*, II, II-59–II-63.

Iliev I., Sirakov E., & Zhivomirov H. (2014). Acoustic Examination of the Anechoic Chamber in Technical University – Varna. *Journal of Acoustics*, XVI (16), 131-138.

Islamov I.J., Aslanzadeh I.A. (2023). Simulation of the Electromagnetic Field of a Microwave Waveguide Taking into Account the Anisotropy of the Medium. *Advanced Physical Research*, 5(3), 168-176.

Islamov I.J., Agayev F.G., & Aliyeva G.V. (2025). Electrodynamic Modeling of a Planar Antenna System for Wireless Communication. *Advanced Physical Research*, 7(1), 87-101.

Islamov I.J., Akhundov R.G., Dimitrov D., & Panevski V. (2025). Modeling of a Circular Disk Monopole Antenna Fed from a Microwave Broadband Coplanar Waveguide. *Advanced Physical Research*, 7(2), 184-195.

Kozien M. (2012). Acoustic Nearfield and Farfield for Vibrating Piston in Geometrical and Intensity Formulations. *Acta Physica Polonica*, 121, A 132-A 135.

Kleiner M. (2013). *Electroacoustics*, Taylor & Francis, 220-221.

Lependin L. (1978). *Acoustics.* Vysshaya Shkola, 265-280 (in Russian).

Rschevkin S. (1960). A Course of Lectures on the Theory of Sound. Moscow University Press, 307-327 (in Russian).

Sirakov E., Iliev I. (2013). Examination of Mechanical Vibration of Circular Piston. *Journal of Acoustics*, *XV*(15), 83-86.

Smith D. (1997). Discrete-Element Line Arrays-Their Modeling and Optimization. *J. Audio Eng. Soc.*, 45, 949-964.

Urban M., Heil C., & Bauman P. (2003). Wavefront sculpture technology. *Journal of the Audio Engineering Society*, 51, 912-932.

Xiong W., Chen W., Li Z., Zhu H., & Wang X. (2025). Effect of Systematic Errors on Building Component Sound Insulation Measurements Using Near-Field Acoustic Holography. *Buildings*, *15*(15), 2619.

Yuning G. (2025). Directional sound propagation in acoustic artificial structures. *npj Acoustics*, *1*(8), 1-19.

Yu, Z., Li, X., Jung, H., Harada, M., Prokhorov, D., & Lee, T. (2024). Robust acoustic directional sensing enabled by synergy between resonator-based sensor and deep learning. *Scientific Reports, 14*(1), 10148.

Zhong C., Lu Q., Li T., Su H., & Liu S. (2024). Real-time acoustic holography with physics-reinforced contrastive learning for acoustic field reconstruction. *J. Appl. Phys.*, 135, 014902.

Zhivomirov H., Iliev I. (2015). Impedance Frequency Response Measurement with Matlab Implementation. *Journal of the Technical University of Gabrovo*, 52, 61-65.